中國造船暨輪機工程學刊第三十八卷第三、四期 民國一〇八年八月
Journal of Taiwan Society of Naval Architects and Marine Engineers, Vol.38, No.3-4, pp.135-155, 2019

APPLYING AN INTELLIGENT PARAMETER DESIGN COMBINED WITH TAGUCHI METHOD ON THE PERFORMANCE OF MULTI-OBJECTIVE OF A PEM FUEL CELL STACK

K. Ouyang[*1] C.-T. Li[**] J.-H. Chang[***]

[*]Department of Marine Engineering, Taipei University of Marine Technology
[**]School of Defense Science, Chung Cheng Institute of Technology, National Defense University
[***]Naval Architecture and Marine Engineering, Chung Cheng Institute of Technology, National Defense University

Keywords: Proton Exchange Membrane Fuel Cell Stack, Taguchi Method, Principal Components Analysis, Backpropagation Neural Network, Multi-objective Optimization

ABSTRACT

This paper presents an approach of the intelligent-robust parameter design to improve the performance of a PEM fuel cell stack with multi-objective cases. Firstly, a screen experiment has to be carried out by using a fractional factorial design; then the Taguchi multi-quality method can be conducted to predict the discrete model; the principal component analysis (PCA) can then be performed on the multi-objectives. The intelligent parameter design is developed via the definition of the percentage reduction of quality loss (PRQL) combined with the S/N ratio models that can be performed by a Backpropagation Neural Network (BPNN), in order to supply a fitness function to the Monte Carlo method. Finally, the prediction model created by this approach can be verified through a confirmation experiment. In this work, a combined approach is employed to determine the optimal combination of five operating parameters that include the temperature of a fuel cell, the anode and cathode humidification temperatures, the stoichiometric flow ratios of the reaction gas etc. for a PEM fuel cell stack. The results indicate that the intelligent parameter design via the average PRQL was improved by 32.35%. However, the Taguchi method and the PCA were improved by 32.03% and 31.61%, respectively.

INTRODUCTION

Over the past several decades, internal combustion engines using fossil fuels have been the main source of power for landed vehicles and commercial ships. However, NOx, SOx, and CO_2 produced by the combustion of fossil fuels cause increasingly serious air pollution and greenhouse effects. Hence, developing the new power source technologies to alternate internal combustion engines is an important issue. Fuel cells convert chemical energy directly into electrical energy through chemical reactions, with the advantage of low emissions and silence [1-2]. Therefore, fuel cell is regarded as an excellent alternative power source in many areas. There are various types of fuel cell, one of them is the Proton Exchange Membrane (PEM) fuel cell, which is described by the use of a polymer electrolyte membrane.

A typical PEM fuel cell consists bipolar plates with gas channel, gas diffusion layers, catalyst layers, and a membrane. PEM fuel cells use hydrogen and oxygen as fuels, water is the reaction product. PEM fuel cells have the characteristics of no electrolyte leakage, short warm-up time, and high specific power [3-5]. It

[1] Corresponding author (f0898@mail.tumt.edu.tw)

can be used not only as a decentralized power supply and for household power, but can also be specifically used as a mobile power supply option, such as for electric vehicles and underwater vehicles [6-8].

The PEMFC system has been used as a suitable power source for an unmanned underwater vehicle conducting long-range underwater surveys and requiring high energy density. In 2005, JAMSTEC demonstrated the autonomous underwater vehicle (AUV) using a PEMFC system that was able to cruise autonomously and continuously for 317 km, which set a world record at that time [9]. Since 2007, the JAMSTEC has started to develop a second-generation fuel cell system for the AUV called the HEML (High efficiency Multi-Less) fuel cell system. Their purpose was to accomplish a system efficiency of over 60%, thus downsizing from the first one by removing a blower and a humidifier on the auxiliaries and reducing hydrogen leakage. They achieved 600 hours of underwater operation by March of 2011 [10]. From the above discussion, it can be assumed that the PEMFC system will be regarded as one of the best AUV power sources and will serve its function fully. Nevertheless, it must be a closed-cycle type in order to run on a continuous supply of pure hydrogen and oxygen from two gas tanks in an underwater environment, then, the PEMFC will always generate electricity in theory. In terms of cruising distances and operating times, the AUV is limited by the capacity of the gas tank it carries. Therefore, applying the multi-objective design in the PEMFC system of the AUV is important to achieve a compromise between fuel economy and the demand for electricity. Our team applied the Taguchi method and metamodeling approach to perform a series of PEMFC studies in the past [11-14]. These studies only concerned a single-objective optimization of fuel cell current density or electrical power. However, more and more studies have been investigating the processing of multi-objective problems for the PEMFC system. Na and Gou [15] employed the MATLAB optimization toolbox for the purpose of solving a cost-efficient model of the PEMFC in order to achieve maximum efficiency and minimum cost goals. Ang et al. [16] presented a multi-objective optimization model using the weighting method for a PEMFC system to improve efficiency and offset the size trade-off problem. Lin et al. [17] used a multi-objective topology optimization model of the end plates in a PEMFC stack to maximize the stiffness of the end plate and unify the pressure distribution at the contact interfaces of the stack at the same time. Peng et al. [18] proposed a multi-objective optimization model for a PEMFC system in order to eliminate the non-uniform distribution in the flow field and take the intrusion of the gas diffusion layer into consideration. Shokuhi-Rad et al. [19] used a uniform-diversity genetic algorithm (MUGA) to perform the optimum design for a PEMFC controller based on three objective functions, which included the minimized integral of the square of error, hydrogen pressure and working temperature. Curteanu et al. [20] developed a multi-objective optimization strategy to combine the stacked neural network with a genetic algorithm and applied it to a high temperature PEMFC system. This approach explored objectives related to the maximum power density as well as the maximum value of the electrochemical active surface area for both an anode and a cathode. Nevertheless, in the studies mentioned above, the analytical parameter effects were not carried out in the experimental designs, and the interactions between the factors were rarely discussed. These interactions may even be sufficient to change the final research conclusions, and the results of some of these experiments therefore probably suffered factor effect bias.

In this paper, an intelligent-robust parameter design combined with the Taguchi method, the principal components analysis (PCA), the backpropagation neural network (BPNN) and the Monte Carlo method are developed and applied on a PEMFC stack. Three objectives, which are three quality characteristics, can achieve a compromise between maximum electric power and minimum pressure drops on the anode and cathode sides for application to undersea vehicles.

In this work, the experiments were carried out based on the Taguchi orthogonal array, and the experimental data were used to design a neural network. The neural network design using the Taguchi experimental data can improve the quality of neural network, can reduce experimental time and cost and can yield results that are more dependable. In addition, the artificial neural network model [21] perfects the Taguchi method model in regard to the discrete factor levels

and therefore complements the drawbacks of the Taguchi method [22]. Finally, the Monte Carlo method searches for the global optimum from the BPNN model.

Furthermore, most applications of the Taguchi method have only dealt with a single-quality problem. However, more than one quality characteristic always takes place in a product design. The Taguchi method via engineering judgment and experience can improve the performance of the product design in the multi-quality problem. Nevertheless, the chosen combination may not be the best due to uncertainty based on the discrete factor levels. Accordingly, a PCA and a percentage reduction of quality loss (PRQL) have been used to optimize a multi-objective problem in this study [23-24]. Finally, the results of the optimum settings are verified by using a confirmation experiment to ensure the accuracy of the predicted model.

This paper is organized as follows: a brief description of a PEMFC stack and an experimental test platform is introduced in Section 2. An effective method proposed in Section 3 consists of the robust design of experiments intended to search the entire data, the BPNN that can be used to establish the experimental model, the Monte Carlo method to seek a global optimal solution for the model, and the PCA and the PRQL that can be applied to optimize the multi-objective problem. The experimental results and discussion of the PEMFC stack from the optimization methods are shown in Section 4. Conclusions from the present study are demonstrated in Section 5. The proposed optimum methodology to improve performance of the PEMFC stack is graphically summarized in Fig. 1.

EXPERIMENTAL SYSTEM

This study considered a test of a PEM fuel cell stack that consisted of five cells, and the active area of each cell was 25 cm^2. The film thickness of the membrane-electrode-assembly (MEA) was 25 μm, and it was the 5510 series from GORE-TEX. The platinum content of the catalyst layer on the anode and cathode sides was 0.4 mg/cm^2. Both sides of the MEA were fitted with gas diffusion layers which is made of carbon paper in the 10 BC series from the SGL Corporation, and the thickness was 0.4 mm. A bipolar plate made of commercial composite carbon with the plate thickness of 3 mm was used, as shown in Fig. 2. Double serpentine flow channels were engraved on the bipolar plate. The width and depth of the anode and cathode channels, and the width of the ribs were all 1 mm (Fig. 2(a)). The other side of the flow channel surface was grooved as straight-through cooling channels; the width was 2 mm, and the depth was 1 mm, to constitute a single cell (Fig. 2(b)). Then five single cells were composed of a stack, and both sides of the five single cells were fitted with gold-plated coppers. Finally, the end plate was made of aluminum alloy 6061 using an anode treatment. All of the parts were fastened using bolts. The operating temperature of the PEMFC stack was regulated by controlling the speed of the cooling fan.

The experimental apparatus of the fuel cell stack (HTS, Hephas Energy Co.) had a gas supply module, a flow rate control module, a temperature control module, a humidifying module, an electronic load module, and an AC impedance module, as shown in Fig. 3. In this study, the mass-flow controllers were regulated with pure hydrogen and air from the gas cylinders under atmospheric pressure and 100% relative humidity (RH). The measurement data were acquired using the constant current density (CC) load mode when the operating conditions were regulated to meet the setting values. The polarization curve data were incrementally

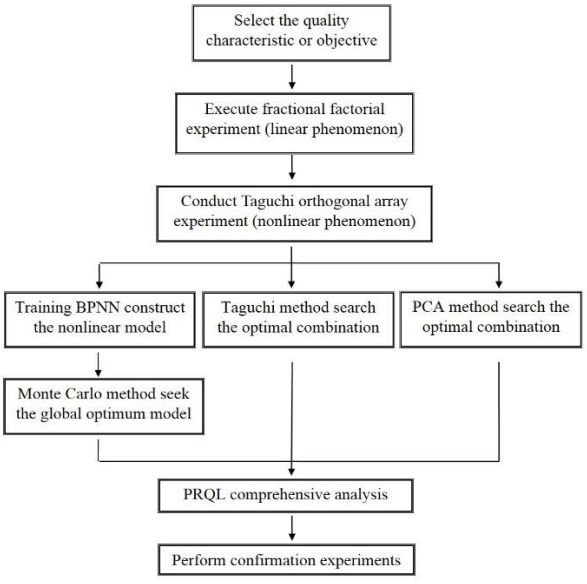

Fig. 1 Flow chart of the optimization methodology.

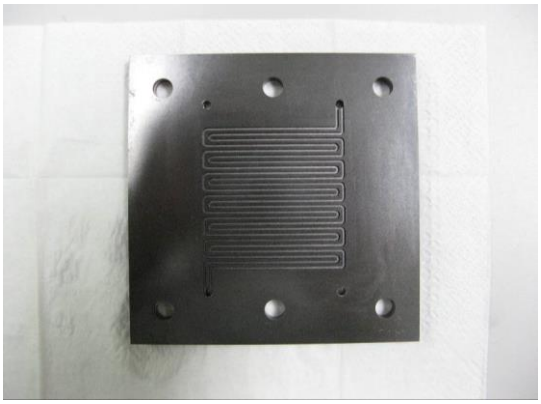

(a) Double serpentine flow channel.

(b) Straight-through cooling channel.

Fig. 2 Bipolar plate of PEM fuel cell.

Fig. 3 Fuel cell test system made by Hephas Energy Corp. Taiwan.

increased by 0.1-25 (mA/cm^2) within the system steady state, and the data averaged over 30 s was recorded using a personal computer.

INTELLIGENT-ROBUST PARAMETER DESIGN

1. Fractional Factorial Experiment

In the 1920s, Fisher, an English statistician, devised the statistical experimental design. The design of experiments (DOE) was applied to agriculture initially; however, now it is being widely used in various fields. In the early stages, most studies that used it extensively in practice were one-factor-at-a-time experiments, but this method had the following flaws: it cannot analyze any possible interactions between factors; each factor may have the different number of occurrences caused by imbalanced experiments; the unmet randomization and orthogonal characteristics could result in missing the optimal factor settings. The factorial experiments were intended to design an experiment to investigate the effect of each factor. If the experimental design took into consideration all factor-level combinations, it would be a full-factorial design.

However, the fractional factorial experiments not only reduced the number of experiments and cut down costs compared to the full-factorial design, but they were also aimed at screening the specified factors in order to determine the effect of the main factor and the interactions occurring between the factors. Then, the selected significant factors and interactions could be arranged in order of priority for further experimentation. Five control factors were considered in our study. Using a 2_V^{5-1} design can reduce the number of runs to 16 times in the case of a fractional factorial design with a resolution V design in which the main effects and the two-factor interactions do not have other main effects and two-factor interactions as their aliases [25]. Most notably, three or more factor interactions are considered to be negligible. In the experimental screening stage, we chose the maximum electric power for the PEMFC stack as the quality characteristic. Therefore, it has a larger-the-better characteristic. The experimental control factors include stack temperature, anode and cathode humidification temperatures, the stoichiometric hydrogen flow ratio, and the stoichiometric

airflow ratio. These control factors and levels were determined from the literature survey and our past studies and satisfy the PEMFC experimental apparatus capacity requirements, as listed in Table 1.

2. Taguchi's Robust Parameter Design

In the 1950s, Taguchi proposed an effective method to improve product quality that is now known as the Taguchi Method. This method adopted a general notion of the statistical method and advocated the application of a proper orthogonal array (OA) to plan experiments. The concept of the loss function was employed by Dr. Taguchi to develop the signal-to-noise ratio (S/N) as the measurable index of characteristic quality. The mean and variance of the quality characteristic can be considered to be a signal and noise, respectively. The maximum S/N is used to decide the optimum factor-level combination. The spirit of this approach is to minimize the impact of various factors for the quality loss, and the product has robustness. Thus, this study considers the nonlinear phenomenon among the five control factors, and the original two levels are subdivided into three levels in the further experimental stage, as shown in Table 2. The selected $L_{27}(3^{13})$ is a proper OA table. Nevertheless, it only runs 27 times in order to adopt the Taguchi method instead of 243 times for a full-factorial experiment. The three quality characteristics of the analytic objective are the maximum electrical power of the stack and minimum pressure drops on both the anode and cathode sides, which belong to the larger-the-better (*LTB*) and the smaller-the-better (*STB*) characteristics, respectively. These formulas are

$$S/N_{LTB} = -10\times\log\frac{1}{n}\left(\sum_{i=1}^{n}\frac{1}{y_i^2}\right) \tag{1}$$

and

$$S/N_{STB} = -10\times\log\frac{1}{n}\left(\sum_{i=1}^{n}y_i^2\right) \tag{2}$$

where y_i refers to the value of the quality characteristic as measured from the trial; the S/N unit is dB, and n is the number of the tests in a trial.

When the optimum factor-level combination is selected from the maximum S/N via the factor response diagram and the ANOVA, the next step is to estimate the performance of the optimal methods. The predicted S/N at the optimum condition is estimated only from the significant factors of the ANOVA analyses. Therefore, the pooled factors are not included in the estimate. The authors adopt the additive modes with interactions due to the interaction between the two factors may exist. The general formula of the predicted mode is determined as shown in the reference [26].

$$\begin{aligned}\hat{\eta}_M(Ai,Bj,Ck,\cdots)\\ =\bar{\eta}_M+(\bar{\eta}_{AiBj}-\bar{\eta}_M)+(\bar{\eta}_{Ck}-\bar{\eta}_M)+\cdots\end{aligned} \tag{3}$$

where *A*, *B*, *C* ... are the significant factors, *i*, *j*, *k* ... are the levels of the significant factors, $\bar{\eta}_M$ is the average S/N for all runs, and $\bar{\eta}_{AiBj}$ is the combination effect.

3. Principal Component Analysis (PCA)

PCA is a common method used in statistics for maximizing the information content in high dimensional data. It was first proposed by Pearson and was later developed by Hotelling. In mathematical terms, PCA finds a set of m orthogonal vectors in the data space that represent the largest variance, and then project the data from their original *n*-dimensional space into the *m*-dimensional subspace, where $m \ll n$,

Table 1 Control factors and levels for the fractional factorial experiment

Factor	Description	Level –1	Level +1
A	Stack temperature (K)	321	337
B	Anode humidification temperature (K)	323	343
C	Cathode humidification temperature (K)	323	343
D	Stoichiometric hydrogen flow ratio λ_{H_2}	1.5	2.5
E	Stoichiometric airflow ratio λ_{air}	2.5	5

Table 2 Control factors and levels for the $L_{27}(3^{13})$ design

Factor	Description	Level 1	Level 2	Level 3
A	Stack temperature (K)	321	329	337
B	Anode humidification temperature (K)	323	333	343
C	Cathode humidification temperature (K)	323	333	343
D	Stoichiometric hydrogen flow ratio λ_{H_2}	1.5	2.0	2.5
E	Stoichiometric airflow ratio λ_{air}	2.5	3.75	5

thereby reducing the data dimensionality. It is a data preprocessing technique that a large number of correlated variables are transformed into a small number of uncorrelated variables, which are called principal components. In our study, an effective procedure based on PCA is used to optimize a multi-quality problem in the Taguchi method. This procedure is capable of decreasing the uncertainty in engineering judgment when the Taguchi's loss function is applied in multi-quality case. The procedure is described as follows [15].

Step 1: Calculate the quality loss for each response, L_{ij}.

Let L_{ij} be loss function for the *i*-th response (or quality characteristic) at the *j*-th trial or experiment run. L_{ij} can be calculated on basis of Taguchi's loss function.

Step 2: Normalize the quality loss for each response.

L_{ij} is transformed into Y_{ij} ($0 \le Y_{ij} \le 1$) by using the following formula

$$Y_{ij} = \frac{L_i^+ - L_{ij}}{L_i^+ - L_i^-} \tag{4}$$

where L_i^+ and L_i^- are the maximum and minimum quality loss for the *i*-th response, respectively. Y_{ij} is the normalized quality loss for the *i*-th response at the *j*-th trial.

Step 3: Perform the principal component analysis (PCA) for Y_{ij}.

Step 4: Determine a small number of principal components, *k*, which account for most of the variance in the original *p* responses, provided that $k \le p$. Then, we calculate linear combination.

$$\Phi_{kj} = \sum_{i=1}^{p} a_{ki} Y_{ij} \tag{5}$$

where a_{k1}, a_{k2}, ... a_{kp} are the elements of the eigenvector corresponding to the *k*-th eigenvalue. Φ_{1j} is referred as the first principal component for the *j*-th experiment trial, which indicates most variance in the data. The second principal component is less, and so on. All the principal components are uncorrelated with each other. In addition, the variances of the principal components are the eigenvalues, and the coefficients of the principal components are referred to as the eigenvectors. It is noted that the sum of the variances of the principal components equals the sum of the variances of the original responses. It is a matter to judge how many components must be considered. The rule of thumb is to choose those components with an eigenvalue greater than or equal to one. The larger the Φ value is, the better the performance of the product becomes.

Step 5: Use the Φ value to determine the optimal factor-level combination. The larger Φ value implies the better quality characteristic and minimum quality loss.

4. Intelligent Parameter Design

4.1 Modeling by Backpropagation Neural Network (BPNN)

In this study, a backpropagation neural network (BPNN) is used as a kind of multilayer feed-forward network architecture; that is, one or more hidden layers between the input and output layer are used to process the function approximation problem. The training algorithm is based on an approximate steepest descent algorithm intended to minimize the mean square error by updating the weights and biases. The backpropagation algorithm is designed to propagate the error backward through the network from the last layer to the first layer and to reduce the error function to improve the precision of the network. Nevertheless, in general, a large amount of the experimental data is not easy to obtain. In order for the training network to have good generalization capability to avoid overfitting, this study adopts Bayesian regularization to train the BPNN, which must be combined with the framework of the Levenberg-Marquardt algorithm.

The MATLAB Neural Network Toolbox is used to construct BPNN modeling in the training function *trainbr* [27]. It provides automated optimal regularization parameters, and its principle is derived from David Mackay's Bayesian techniques. The performance function is

$$F_p = \beta SS_E + \alpha SS_W \tag{6}$$

where SS_E is the sum squared errors, and SS_W is the sum squared weights of the network; α and β are performance function parameters. If $\alpha << \beta$, the training algorithm will make the errors smaller. If

$\alpha >> \beta$, the training will decrease the weighting size at the expense of network errors, thus generating a smoother network response to avoid possible overfitting phenomenon [28]. Furthermore, the best results are acquired if the raw training data is normalized into the range [−1, 1] by the following equation

$$y_n = 2\times\frac{y-y_{\min}}{y_{\max}-y_{\min}}-1 \tag{7}$$

where y_n is the normalized data; y is the raw data, and $y_{\max}$ and $y_{\min}$ are the maximum and minimum values of the raw data, respectively.

Another approach for improving network generalization is called early stopping. The raw data must be divided into three subsets: a training set, a validation set, and a test set. The training set is utilized for calculating the gradient and updating the network weights and biases. The error on the validation set is monitored during the training course. The test set error is not used during training, but it is used to compare different models and verify data division at random. Consequently, early stopping and regularization can ensure network generalization when they are applied properly. Finally, in order to determine the error between the predicted and experimental data, the coefficient of determination (R^2) and the root mean square error (RMSE) are adopted according to reference [29],

$$R^2 = 1-\frac{\sum_{i=1}^{n}\left(y_i-\hat{y}_i\right)^2}{\sum_{i=1}^{n}\left(y_i-\bar{y}\right)^2} \tag{8}$$

$$RMSE = \sqrt{\frac{1}{n}\sum_{i=1}^{n}\left(y_i-\hat{y}_i\right)^2} \tag{9}$$

where n is the number of data pairs; $\bar{y}$ is the mean of the observed value; y_i and $\hat{y}_i$ are the i-th observed value and predicted value, respectively. The values of the R^2 approximated to 1 imply that the model has strong predictive ability. The smaller *RMSE* values indicate better performance.

4.2 Optimization by Monte Carlo Method

The Monte Carlo method depends on repeated random sampling to obtain a great deal of numerical data by applying computer simulations. The name comes from gambling, where playing and recording is done as in an actual Monte Carlo Casino. The Monte Carlo method is usually used in physical and mathematical problems when it is either hard or impossible to acquire a closed-form expression or a deterministic algorithm. Nowadays, the Monte Carlo method is mainly applied in scopes including optimization, a numerical integration and a drawing generation from a probability distribution, among others. Therefore, in this study, the Monte Carlo method is used as well as the evolutionary strategy optimization. We generate random inputs by using the scattering grains over the BPNN model and then perform a computation with a fitness function on each input. In addition, for the sake of increasing accuracy, we introduce a concept of a bomb effect and generate offspring parameters to add tiny, moderate and large random disturbances. This is similar to the mutation operator of a genetic algorithm (GA). Finally, a convergence criterion of the optimal value gradually decreases the scope of the computational domain. This approach uses a purely numerical optimization procedure, which is similar to a focused Monte Carlo search [30]. In addition, when we use this approach, we do not need to represent the problem in a coded form. The hardest part of applying a GA is coding the problem. Then, we calculate the fitness function by using an array type. This method can obtain a global optimal solution quickly. A flowchart of the Monte Carlo method is shown in Fig. 4.

4.3 Percentage Reduction of Quality Loss (PRQL)

Maghsoodloo described the exact relation of the S/N and the quality loss function. He then proposed a relation of the percentage reduction of quality loss (PRQL) and mean square deviation [31]. Taguchi defined the average quality loss as

$$L = k\times MSD \tag{10}$$

where L is the present existing average loss per unit; k is the loss coefficient, and *MSD* is the sample mean square deviation

$$MSD = \begin{cases} \dfrac{1}{n}\sum_{i=1}^{n} y_i^2 & \text{for STB} \\ \dfrac{1}{n}\sum_{i=1}^{n}\dfrac{1}{y_i^2} & \text{for LTB} \end{cases} \tag{11}$$

where n units of a product are measured; y is a measurable statistic of quality characteristic, and $\bar{y}$ is the sample mean of n units. For cases concerning the *STB*

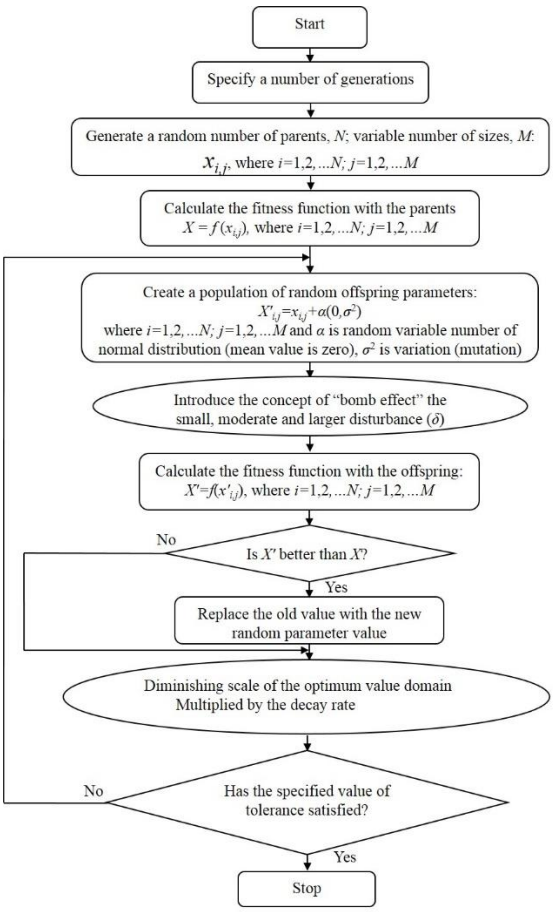

Fig. 4 Flow chart of the Monte Carlo method.

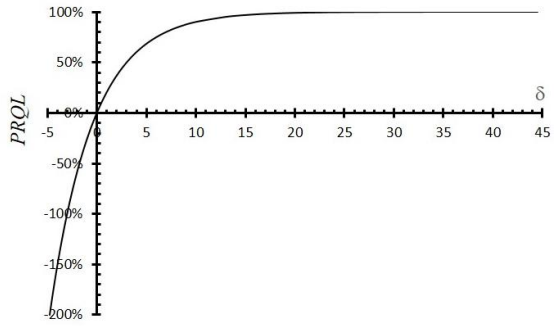

Fig. 5 δ-*PRQL* relationship diagram.

and the *LTB* quality characteristics, Taguchi's S/N is defined as $\eta = -10\times\log_{10}(MSD)$. Substituting into Eq. (10), we can obtain

$$\eta = -10\times\log_{10}(MSD) = \log_{10}\left(\frac{k}{L}\right)^{10} \tag{12a}$$

or

$$L = k\times(MSD) = k\times 10^{-\frac{\eta}{10}} \tag{12b}$$

Suppose L and L' are the loss functions of the product for the original and new parametric designs, respectively, after the parameter design the S/N has changed from an existing η to another value η'; that is, in accordance with Eq. (12): $L' = k\times 10^{-\eta'/10}$. Thus, we acquire the percentage reduction of quality loss (PRQL) to be

$$\begin{aligned}\text{Max: PRQL} &= \frac{L-L'}{L}\times 100\% \\ &= \left[1-\frac{k(10^{-\frac{\eta'}{10}})}{k(10^{-\frac{\eta}{10}})}\right]\times 100\% \\ &= (1-10^{-\frac{\delta}{10}})\times 100\%\end{aligned} \tag{13}$$

where $\delta = \eta' - \eta$ is the S/N difference between the original and new parametric designs. Suppose there are n control factors X_1, X_2, ..., X_n in which the *STB* has i outputs and the *LTB* has j outputs. The purpose of the parameter design for this study with multi-quality characteristics is to minimize the total quality loss (TQL); that is

$$\begin{aligned}\text{Min: } & L_{TQL}(X_1, X_2, \cdots, X_n) \\ &= \sum_{a=1}^{i} L_{STB_a}(X_1, X_2, \cdots, X_n) \\ &\quad + \sum_{b=1}^{j} L_{LTB_b}(X_1, X_2, \cdots, X_n)\end{aligned} \tag{14}$$

where the L is quality loss function, the subscript *TQL* represents the total quality loss, *STB* and *LTB* are the quality losses for the-smaller-the-better and the-larger-the-better terms, respectively. When the δ increases 3dB, the quality loss of a product decreases 50% by Eq. (12), as shown in Fig. 5. Consequently, this study applied the TQL, which is regarded as a fitness function of the Monte Carlo method, in order to evaluate the average percentage reduction of quality loss (*APRQL*).

$$\begin{aligned}&APRQL \\ &= \frac{1}{3}\left(PRQL_{power} + PRQL_{anode} + PRQL_{cathode}\right)\end{aligned} \tag{15}$$

where $PRQL_{power}$, $PRQL_{anode}$, and $PRQL_{cathode}$ represent the *PRQL* of electrical power and the pressure drops on the anode and cathode sides, respectively. This approach provides an optimal parameter design

Table 3 The Experimental Data with Stack Current Density of 500 mA/cm^2 for the 2_V^{5-1} Design

Trial no.	Control factors					Power (Watt)			Avg. (Watt)
	A	B	C	D	E	R_1	R_2	R_3	
1	–1	–1	–1	–1	1	42.80	43.00	42.80	42.87
2	1	–1	–1	–1	–1	42.59	42.80	42.59	42.66
3	–1	1	–1	–1	–1	41.76	41.76	41.76	41.76
4	1	1	–1	–1	1	44.05	43.96	44.05	44.02
5	–1	–1	1	–1	–1	41.96	41.76	41.76	41.83
6	1	–1	1	–1	1	43.88	43.88	43.63	43.80
7	–1	1	1	–1	1	43.63	43.63	43.63	43.63
8	1	1	1	–1	–1	43.00	43.00	43.33	43.11
9	–1	–1	–1	1	–1	41.76	41.76	41.51	41.68
10	1	–1	–1	1	1	42.39	42.59	42.39	42.46
11	–1	1	–1	1	1	43.63	43.43	43.43	43.50
12	1	1	–1	1	–1	43.00	43.00	43.00	43.00
13	–1	–1	1	1	1	43.43	43.43	43.24	43.37
14	1	–1	1	1	–1	42.59	42.59	42.39	42.52
15	–1	1	1	1	–1	41.96	41.96	42.39	42.11
16	1	1	1	1	1	43.63	43.63	43.43	43.56

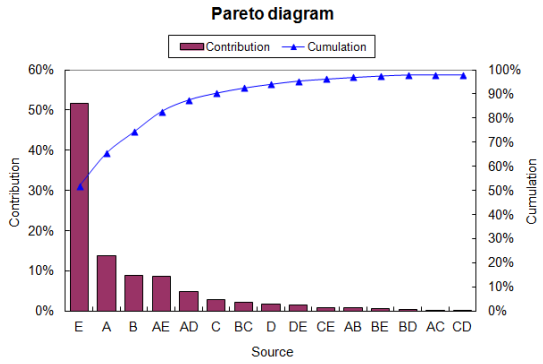

Fig. 6 Pareto chart of factors for the fractional factorial experiment.

that transforms three quality characteristics into a single one that is equal to the traditional Taguchi method to maximize the *PRQL* value. Then, an intelligence parameter design can be performed for the metamodeling optimization by combining the backpropagation neural network and the Monte Carlo method (BPNN-MC).

RESULTS AND DISCUSSION

1. Fractional Factorial Design and Analysis

A 2_V^{5-1} combination table with a resolution *V* design is used in the present study. Each experimental combination has three repeated measuring data under a PEMFC stack current density of 500 mA/cm^2, as shown in Table 3. An average value obtained from the measured data could be analyzed by the well-known technique of Yates's rule. This rule allows for estimating the effect of all main factors and all two-factor interactions quickly. Fig. 6 presents the Pareto chart results for the screening experiment. Therefore, the influence ranks of significant factors with the maximum electrical power are as follows: stoichiometric airflow ratio (E), stack temperature (A), the anode humidification temperature (B), the interaction of stack temperature and stoichiometric airflow ratio (A×E), the interaction of stack temperature and stoichiometric hydrogen flow ratio (A×D), and the cathode humidification temperature (C). From the results mentioned above, a cumulative contribution of the six significant factors and interactions reached more than 90% of the overall contribution. They can be regarded as the important factors and interactions. The interaction response diagrams of the A×E and A×D are considered significant interactions as shown in Fig. 7. Note that the A_{-1} and A_{+1} lines as well as the D_{-1} and D_{+1} lines are not parallel. This indicates the interactions between factors A and E, A and D. Consequently, the E, A, and D factors are prioritized to be arranged in the column positions in a subsequent Taguchi OA experiment because the

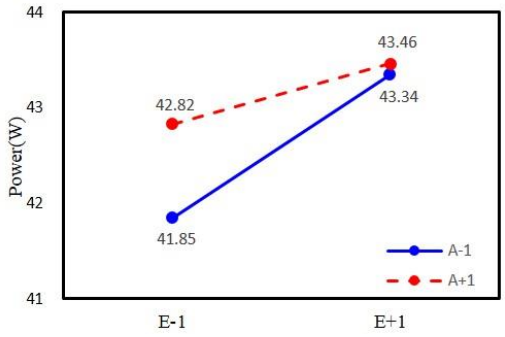

(a) A×E.

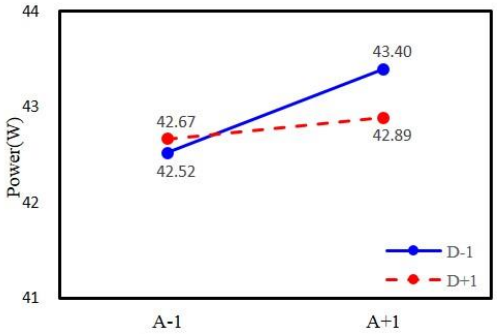

(b) A×D.

Fig. 7 Interaction graph for the fractional factorial experiment.

interaction relationships were shown to exist.

2. Optimization of Taguchi Multi-quality Method

In general, Taguchi method can only process the optimization of a single quality characteristic, and that is one objective at a time. In this study, the $L_{27}(3^{13})$ table of the Taguchi method was applied to acquire the optimum factor-level combination for the PEMFC stack. Moreover, its purpose became a compromise of three quality characteristics among the maximum electrical power, and the minimum pressure drops on both the anode and cathode sides under different PEMFC stack operating conditions. As seen from Table 4, the S/N values of the maximum electrical power and the minimum pressure drops on both the anode and cathode sides are calculated by Eqs. (1) and (2), respectively. The main factor-response graph and the ANOVA results for the analytical data for the three quality characteristics are shown in Fig. 8 and Table 5, respectively. Table 5(a) presents the ANOVA results with a 99% confidence level, the critical value of main

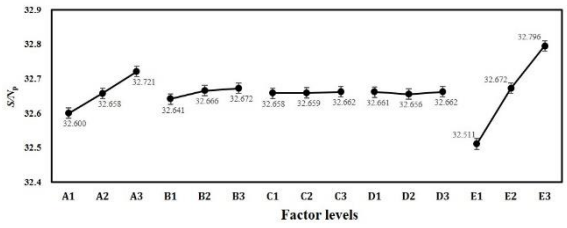

(a) Electrical power.

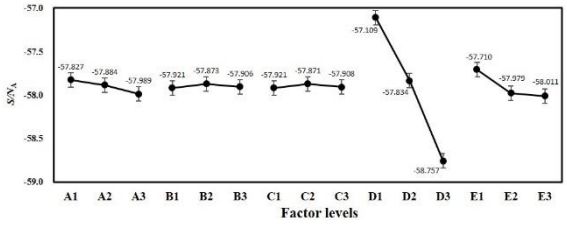

(b) Pressure drop on the anode side.

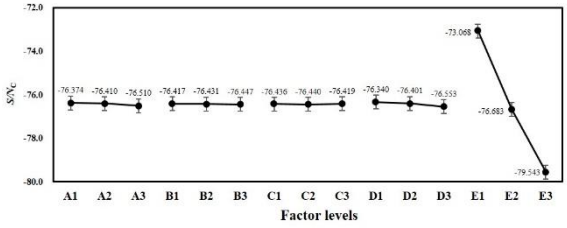

(c) Pressure drop on the cathode side.

Fig. 8 S/N response of three quality characteristics for the $L_{27}(3^{13})$ design.

factors $F_{0.01}$ is 6.226 and interactions between the factors F0.01 is 4.773. When the F-test value of main factors is smaller than 6.226 and interactions between the factors is smaller than 4.773, it means insignificant and pools them as errors. Therefore, the factors with significant effect for acquiring maximum electrical power are as follows: stoichiometric airflow ratio (E), stack temperature (A), the anode humidification temperature (B), and the interaction of stack temper-ature and stoichiometric airflow ratio (A×E). The initial optimal levels of the significant factors, A_3, B_3, and E_3, can be determined from Fig. 8(a). As shown in Table 5(b) and (c), the ANOVA results indicate that the significant factors are factor A, D, E and D×E for minimum pressure drop on both anode and cathode sides. Referring to Figs. 8(b) and (c), the optimal factor level for the quality characteristic of the minimum pressure drops on both the anode and cathode sides are shown as A_1, D_1, E_1 and A_1, D_2, E_1, respectively. These results reveal that a factor may be acquire different optimal

Table 4 The Experimental Data with Stack Current Density of 500 mA/cm^2 for the $L_{27}(3^{13})$ Design

Trial no.	A	E	A×E	A×E	D	A×D	A×D	D×E	B	C	D×E	e	e	Power (W)			S/N_p (dB)	Pressure drop on the anode (Pa)			S/N_A (dB)	Pressure drop on the cathode (Pa)			S/N_c (dB)
														y_1	y_2	y_3		y_1	y_2	y_3		y_1	y_2	y_3	
1	1	1	1	1	1	1	1	1	1	1	1	1	1	41.51	41.76	41.76	32.40	695	688	690	-56.79	4473	4434	4466	-72.98
2	1	1	1	1	2	2	2	2	2	2	2	2	2	41.76	41.76	41.96	32.43	716	729	731	-57.21	4426	4462	4450	-72.96
3	1	1	1	1	3	3	3	3	3	3	3	3	3	41.96	41.96	42.19	32.47	872	866	854	-58.73	4492	4461	4501	-73.03
4	1	2	2	2	1	1	1	2	2	2	3	3	3	42.71	42.80	42.71	32.61	714	739	729	-57.24	6680	6701	6699	-76.51
5	1	2	2	2	2	2	2	3	3	3	1	1	1	42.80	42.71	42.80	32.62	797	769	781	-57.87	6916	6576	6899	-76.65
6	1	2	2	2	3	3	3	1	1	1	2	2	2	42.71	42.71	42.71	32.61	863	848	860	-58.66	6892	6904	6879	-76.77
7	1	3	3	3	1	1	1	3	3	3	2	2	2	43.48	43.48	43.52	32.77	697	723	731	-57.11	9250	9201	9191	-79.29
8	1	3	3	3	2	2	2	1	1	1	3	3	3	43.24	43.48	43.24	32.73	816	799	801	-58.12	9467	9511	9494	-79.55
9	1	3	3	3	3	3	3	2	2	2	1	1	1	43.48	43.43	43.48	32.76	847	866	873	-58.71	9588	9543	9609	-79.63
10	2	1	2	3	1	2	3	1	2	3	1	2	3	42.24	42.24	42.59	32.54	706	688	690	-56.84	4545	4434	4466	-73.03
11	2	1	2	3	2	3	1	2	3	1	2	3	1	42.24	42.04	42.24	32.50	740	759	766	-57.56	4486	4462	4450	-73.00
12	2	1	2	3	3	1	2	3	1	2	3	1	2	42.04	42.04	42.24	32.49	885	866	854	-58.77	4554	4461	4501	-73.07
13	2	2	3	1	1	2	3	2	3	1	3	1	2	43.22	43.00	43.22	32.70	723	739	729	-57.27	6761	6701	6699	-76.55
14	2	2	3	1	2	3	1	3	1	2	1	2	3	43.00	43.00	43.00	32.67	808	769	781	-57.91	6970	6576	6899	-76.67
15	2	2	3	1	3	1	2	1	2	3	2	3	1	43.22	43.00	43.00	32.68	875	848	860	-58.70	6962	6904	6879	-76.80
16	2	3	1	2	1	2	3	3	1	2	2	3	1	43.48	43.48	43.53	32.77	705	723	731	-57.14	9321	9201	9191	-79.31
17	2	3	1	2	2	3	1	1	2	3	3	1	2	43.52	43.52	43.63	32.78	789	799	801	-58.02	9539	9511	9494	-79.57
18	2	3	1	2	3	1	2	2	3	1	1	2	3	43.63	43.63	43.52	32.79	860	866	873	-58.75	9656	9612	9669	-79.69
19	3	1	3	2	1	3	2	1	3	2	1	3	2	42.80	42.59	42.59	32.60	717	698	699	-56.96	4602	4589	4595	-73.25
20	3	1	3	2	2	1	3	2	1	3	2	1	3	42.59	42.59	42.39	32.57	753	766	775	-57.67	4439	4465	4445	-72.97
21	3	1	3	2	3	2	1	3	2	1	3	2	1	42.80	42.59	42.59	32.60	893	877	862	-58.86	4611	4634	4666	-73.32
22	3	2	1	3	1	3	2	2	1	3	3	2	1	43.24	43.24	43.00	32.70	730	748	737	-57.37	6825	6801	6843	-76.68
23	3	2	1	3	2	1	3	3	2	1	1	3	2	43.24	43.24	43.43	32.73	816	781	790	-58.02	6729	6785	6755	-76.60
24	3	2	1	3	3	2	1	1	3	2	2	1	3	43.43	43.24	43.24	32.73	883	855	868	-58.77	7044	7002	6998	-76.92
25	3	3	2	1	1	3	2	3	2	1	2	1	3	43.96	43.96	43.88	32.86	716	730	744	-57.26	9399	9421	9381	-79.46
26	3	3	2	1	2	1	3	1	3	2	3	2	1	44.04	43.96	44.04	32.87	802	811	808	-58.13	9587	9600	9595	-79.64
27	3	3	2	1	3	2	1	2	1	3	1	3	2	43.88	43.88	43.63	32.83	876	871	883	-58.86	9731	9712	9696	-79.75

Table 5 ANOVA for the $L_{27}(3^{13})$ Design

(a) Electrical power

Factor	*SS*	*DOF*	*Var*	*F*-test	$F_{0.01}$	P	*SS'*	Contribution
A	0.0648	2	0.0324	200.777	6.226	4.65E-12	0.0645	14.51%
B	0.0050	2	0.0025	15.588	6.226	1.75E-04	0.0047	1.06%
C	(0.0002)	(2)	—	—	—	—	—	—
D	(0.0002)	(2)	—	—	—	—	—	—
E	0.3670	2	0.1835	1137.240	6.226	5.67E-18	0.3667	82.54%
A×D	(0.0013)	(4)	—	—	—	—	—	—
A×E	0.0048	4	0.0012	7.499	4.773	1.33E-03	0.0042	0.94%
D×E	(0.0004)	(4)	—	—	—	—	—	—
Error	0.0026	16	0.0002				0.0042	0.94%
Total	0.4443	26		(At least 99% confidence level)			762.17	100%

(b) Pressure drop on the anode side

Factor	*SS*	*DOF*	*Var*	*F*-test	$F_{0.01}$	P	*SS'*	Contribution
A	0.1244	2	0.0622	13.184	6.226	4.14E-04	0.1150	0.86%
B	(0.0107)	(2)	—	—	—	—	—	—
C	(0.0112)	(2)	—	—	—	—	—	—
D	12.3070	2	6.1535	1304.352	6.226	1.91E-18	12.2976	91.66%
E	0.4943	2	0.2471	52.386	6.226	9.49E-08	0.4848	3.61%
A×D	(0.0056)	(4)	—	—	—	—	—	—
A×E	(0.0253)	(4)	—	—	—	—	—	—
D×E	0.4158	4	0.1039	22.034	4.773	2.41E-06	0.3969	2.96%
Error	0.0755	16	0.0047				0.1227	0.91%
Total	13.4169	26		(At least 99% confidence level)			762.17	100%

(c) Pressure drop on the cathode side

Factor	*SS*	*DOF*	*Var*	*F*-test	$F_{0.01}$	P	*SS'*	Contribution
A	0.0882	2	0.0441	11.100	6.226	9.47E-04	0.0803	0.04%
B	(0.0039)	(2)	—	—	—	—	—	—
C	(0.0025)	(2)	—	—	—	—	—	—
D	0.2176	2	0.1088	27.367	6.226	6.85E-06	0.2096	0.11%
E	189.4301	2	94.7151	23828.26	6.226	1.61E-28	189.4222	99.75%
A×D	(0.0407)	(4)	—	—	—	—	—	—
A×E	(0.0087)	(4)	—	—	—	—	—	—
D×E	0.1017	4	0.0254	6.394	4.773	2.85E-03	0.0858	0.05%
Error	0.0636	16	0.0040				0.1033	0.05%
Total	189.9012	26		(At least 99% confidence level)			189.9012	100%

levels for different quality characteristics.

In this study, the ANOVA contributions of factors and interactions between the factors are smaller than 1%, and these classified as insignificant factors and thus regarded as errors. It will be easy to assist the Taguchi multi-quality method in the engineering judgment. Therefore, based on the ANOVA contribution and significance of the factor effects in the engineering

Table 6 The optimum combination for the Taguchi multi-quality method

Optimum Condition	A	B	C	D	E
S/N_P	A_3	B_3	—	—	E_3^*
S/N_A		—	—	D_1^*	E_1
S/N_C		—	—		E_1^*
Taguchi Method	A_3	B_3	C_2	D_1	E_1

* important

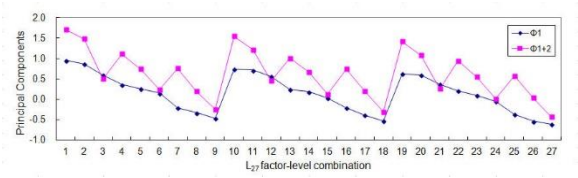

Fig. 9 Comparison of the linear combinations with the first principal component Φ_1, and the first combined with the second principal component Φ_{1+2}.

judgment, the key factors are marked with the important symbol, as shown in Table 6. The levels of the A, B, and D factor (stack temperature, anode humidification temperature, and stoichiometric hydrogen flow ratio) have A_3, B_3, and D_1 as a significant option. There is not a significant option for the C factor (cathode humidification temperature) with the three quality characteristics. For that reason, the level of the C2 with the optimum S/N of electrical power selected from the OA trial No. 26 is treated as the starting condition to acquire of the maximum electrical power with a single objective. Thus, C_2 is selected as the best option. The E factor (stoichiometric airflow ratio) levels are E_3, E_1 and E_1, as shown in Table 6. By most decisions, E_1 is the best selection. Consequently, the Taguchi method in the engineering judgment arrives at a compromise between maximum electrical power and minimum pressure drops on both the anode and cathode sides. The optimal combination is set as $A_3B_3C_2D_1E_1$ via a comprehensive analysis. Unfortunately, the Taguchi multi-quality method in the engineering judgment increases the uncertainty during the decision-making process. In addition, the selected combination with the Taguchi optimization may not necessarily be the best choice on the discrete factor levels. For this reason, the consequences must be verified by using the PCA and the intelligent parameter design described in the next section.

3. Optimization of PCA

One factor significant in a single-response problem may not be significant to the other quality characteristics when considered in a multi-response problem. An effective procedure (*Principal Component Analysis* section) contains the Taguchi's loss function and the PCA to achieve the optimization of multi-objective problem. First, the multi-objective array from the mean square deviation of each trial was normalized using Eq. (4). The results are listed in Table 7. The PCA can be performed in MINITAB software to obtain the Eigenvalues and Eigenvectors of each principal component, as shown in Table 8. Based on Kasier's criterion [32], the componential eigenvalues greater than 1 are selected to replace the original responses. However, the eigenvalues of the first principal component are greater than 1, but the variable proportion is only 65.6%. Furthermore, linear combinations of the first and second principal components for the system variance are higher than the first principal component; this comparison is shown as Fig. 9. Consequently, the first combined with the second principal components that correspond to the two eigenvalues are considered, and the cumulative proportion is 96.3% of the total variance. The eigenvector for the first largest eigenvalue is [−0.680066, 0.275649, 0.679358]. The eigenvector of the second principal component is [0.192078, 0.961250, −0.197748]. As a result, we obtain the linear combinations for the first and second principal component (Φ_{1+2}) using Eq. (5),

$$\begin{aligned}&\Phi_{1j}+\Phi_{2j}\\&=\left(-0.680066Y_{1j}+0.275649Y_{2j}+0.679358Y_{3j}\right)\\&\quad+\left(0.192078Y_{1j}+0.961250Y_{2j}-0.197748Y_{3j}\right)\end{aligned} \tag{16}$$

where Y_{1j}, Y_{2j}, and Y_{3j} represent the normalized quality loss for the responses electrical power and pressure drops on both the anode and cathode sides at *j*-th trial respectively. The Φ_{1+2} values are computed and listed in the last column of Table 7. Based on the results of the main response graph (Fig. 10) and the ANOVA (Table. 9) for the Φ_{1+2} values, the larger the Φ_{1+2} value implies the better the quality. The factors with the significant effect for three quality characteristics are as follows: stoichiometric hydrogen flow ratio (D), stoichiometric airflow ratio (E), stack temperature (A), and the interaction of stoichiometric hydro-

gen flow ratio and stoichiometric airflow ratio ($D \times E$). The initial optimal levels of the significant factors, D_1, E_1, and A_1, can be determined from Fig. 10. Nevertheless, there are insignificant options for the B and C factor (anode and cathode humidification temperature). In the Taguchi method, the factors without any significant effects on the reaction of the PEMFCs are set as constants with a favorable level. Thus, the levels of the insignificant factors, B and C, can be set as B_1 and C_2 from cost consideration and the higher Φ_{1+2} value, respectively. Consequently, the optimum factor-level combination is $A_1B_1C_2D_1E_1$.

4. Optimization of Intelligent Parameter Design

The BPNN is the most popular tool for intelligent systems modeling. The stack temperature, anode and cathode humidification temperature, stoichiometric hydrogen flow ratio, and stoichiometric airflow ratio are set as five input parameters, while the maximum electrical power of the PEMFC stack and the minimum pressure drops on both the anode and cathode sides are set as three output parameters. However, we only have 27 training sets from the Taguchi experimental design. In order to increase the generalization of the BPNN model, we derive the S/N of the prediction equation for the electrical power and the pressure drops on the anode and cathode sides, which are also called the additive modes with interactions by using Eq. (3),

$$\eta_{\text{Power}} = \bar{\eta}_{B_3} + \bar{\eta}_{A_3E_1} - \bar{\eta} \tag{17}$$

$$\eta_{\Delta P(\text{anode})} = \bar{\eta}_{A_3} + \bar{\eta}_{D_1E_1} \tag{18}$$

$$\eta_{\Delta P(\text{cathode})} = \bar{\eta}_{A_3} + \bar{\eta}_{D_1E_1} \tag{19}$$

Table 7 The normalized quality characteristics and the linear combinations of the principal components

Exp.	Normalization			Principal Components	
	Y_{Power}	$Y_{Anode\ P.D.}$	$Y_{Cathode\ P.D.}$	Φ_1	Φ_{1+2}
1	0	1	0.99860624	0.95406028	1.71783787
2	0.07026476	0.83356495	1	0.86134476	1.47835739
3	0.16562432	0.07976488	0.9953686	0.58556321	0.49721785
4	0.47551699	0.82341849	0.6643176	0.35490096	1.10638102
5	0.48898758	0.53934832	0.6452379	0.25447442	0.73925241
6	0.46204641	0.12101538	0.6281881	0.14590017	0.22675235
7	0.79138858	0.87410406	0.12663839	-0.2112179	0.75598075
8	0.72055317	0.41470986	0.05725064	-0.3368159	0.18890545
9	0.77857621	0.09135008	0.03440028	-0.4809328	-0.2503775
10	0.30774757	0.98243066	0.99570405	0.73795691	1.54453152
11	0.22688587	0.68310204	0.99760994	0.71173333	1.21466962
12	0.19740167	0.05372495	0.99286173	0.55507156	0.44829478
13	0.64906164	0.8086742	0.65945129	0.22950887	1.00111245
14	0.58756058	0.51922071	0.64188628	0.17961314	0.66463996
15	0.61831111	0.09723845	0.62385343	0.03013092	0.11899977
16	0.79274672	0.86131724	0.12074485	-0.21967	0.7366636
17	0.81784608	0.46411401	0.0511341	-0.3935186	0.19958984
18	0.83232971	0.06605119	0.01747349	-0.5359617	-0.3160529
19	0.44115443	0.93453252	0.98189784	0.62464894	1.41353618
20	0.3811528	0.63299333	0.99956397	0.59433665	1.07835088
21	0.44115443	0	0.97673312	0.36353717	0.25512631
22	0.65460615	0.76845089	0.64081355	0.20198901	0.93967849
23	0.71372774	0.46708499	0.65294974	0.08695598	0.54391354
24	0.71372774	0.05185412	0.60524747	-0.059909	0.00734094
25	0.9694403	0.81004112	0.08013415	-0.3815568	0.56745735

Φ_1 : the linear combination of the first principal component

Φ_{1+2} : the linear combination of the first and second principal components

Table 8 The normalized quality characteristics and the linear combinations of the principal components

		PC_1	PC_2	PC_3
Proportion		65.6%	30.7%	3.7%
Cumulative		65.6%	96.3%	100%
Eigenvalues		1.9677	0.9204	0.1119
Eigenvectors	Y_P	–0.680066	0.192078	0.707542
	Y_A	0.275649	0.961250	0.003992
	Y_C	0.679358	–0.197748	0.706660

Table 9 ANOVA for Φ_{1+2}

Factor	*SS*	*DOF*	*Var*	F-test	$F_{0.01}$	P	*SS'*	Contribution
A	0.2399	2	0.1200	49.932	6.226	1.32E-07	0.2351	2.62%
B	(0.0036)	(2)	—	—	—	—	—	—
C	(0.0036)	(2)	—	—	—	—	—	—
D	4.8096	2	2.4048	1000.986	6.226	1.56E-17	4.8048	53.64%
E	3.7187	2	1.8594	773.944	6.226	1.20E-16	3.7139	41.46%
A×D	(0.0017)	(4)	—	—	—	—	—	—
A×E	(0.0227)	(4)	—	—	—	—	—	—
D×E	0.1515	4	0.0379	15.767	4.773	2.08E-05	0.1419	1.58%
Error	0.0384	16	0.0024				0.0625	0.70%
Total	8.9582	26		(At least 99% confidence level)			8.9582	100%

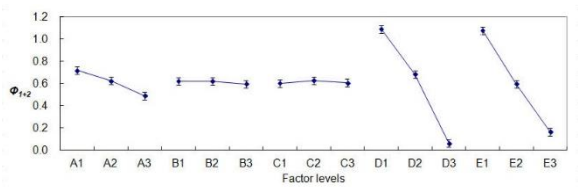

Fig. 10 Linear combination response of main factors for the first combined with the second principal component.

where $\bar{\eta}$ is the mean value of all experimental S/N. Applying the above three equations, we can build the 48 validation sets from the predicted additive modes with the exception of the $L_{27}(3^{13})$ OA combinations, and we can combine an early stopping strategy to train the network model. The initial number of hidden nodes can be evaluated by Eq. (20), as shown in reference [33],

$$N_{\text{Hidden}} = \frac{\text{Number of input nodes} + \text{Number of output nodes}}{2} + \sqrt{\text{Number of training samples}} \quad (20)$$

For this study, the number of hidden nodes approximates 9 as an initial setup. Table 10 presents the performance indices of the BPNN training architectures. We selected a 5-9-3 training architecture, using the smallest RMSE difference between the training set and the validation set. In addition, to verify the accuracy and trends of the BPNN model, the significant interactions via the *F*-test of the ANOVA are selected. The interaction graphs for the three quality characteristics of electrical power and pressure drops on the anode and cathode sides are built by using the Taguchi method in order to compare the results with the BPNN model, as shown in Fig. 11. When the Taguchi method model is compared with the BPNN model, we can see the similar trends and the overlap of the confidence intervals. Therefore, the resulted network for the 5-9-3 training architecture has good generalization capability. The intelligent parameter design combines the BPNN model with the Monte Carlo method to seek the global optimum. Fig. 12 displays the APRQL effects of the A×E and the D×E interaction with the three quality characteristics. The yellow point in Fig. 12 is the optimum factor-level combination according to the BPNN-MC optimization at a stack temperature of 325.75 K, an anode humidification temperature of 343

Table 10 Performance parameters of the BPNN training architectures

Network architectures	R			R^2			SSE	Num Parameters	Sum Squared Param	RMSE for training	RMSE for validation	Difference
5-7-3_nn1	0.9933	0.9846	0.9996	0.9865	0.9676	0.9992	0.524	39.8/66	7.65	0.127714	0.127442	0.000272
5-7-3_nn2	0.9944	0.9874	0.9966	0.9884	0.9725	0.9991	0.449	47.0/66	9.42	0.116919	0.115085	0.001834
5-8-3_nn1	0.9952	0.9884	0.9994	0.9903	0.9746	0.9988	0.413	49.5/75	9.90	0.116971	0.120853	0.003882
5-8-3_nn2	0.9950	0.9882	0.9995	0.9900	0.9753	0.9989	0.405	48.4/75	9.59	0.116236	0.115659	0.000577
5-9-3_nn1	0.9936	0.9890	0.9994	0.9866	0.9766	0.9971	0.508	42.1/84	7.37	0.122033	0.122035	0.000002
5-9-3_nn2	0.9936	0.9864	0.9996	0.9873	0.9720	0.9992	0.462	48.9/84	9.47	0.120267	0.119807	0.000460
5-10-3_nn1	0.9938	0.9853	0.9996	0.9876	0.9693	0.9990	0.498	42.7/93	7.34	0.124275	0.122829	0.001446
5-10-3_nn2	0.9945	0.9877	0.9997	0.9889	0.9845	0.9991	0.421	48.2/93	8.96	0.115020	0.115268	0.000248
5-11-3_nn1	0.9931	0.9811	0.9996	0.9849	0.9609	0.9977	0.645	42.8/102	7.47	0.143116	0.142238	0.000879
5-11-3_nn2	0.9937	0.9867	0.9996	0.9873	0.9723	0.9990	0.462	48.7/102	9.45	0.120148	0.119296	0.000852
5-12-3_nn1	0.9949	0.9863	0.9994	0.9896	0.9714	0.9987	0.459	48.8/111	9.50	0.125020	0.123806	0.001215
5-12-3_nn2	0.949	0.9864	0.9996	0.9893	0.9714	0.9985	0.466	43.3/111	7.82	0.125621	0.124915	0.000706

K, a cathode humidification temperature of 342.9 K, a stoichiometric hydrogen flow ratio of 1.5, and a stoichiometric airflow ratio of 2.5. In a single-objective case, OA trial No. 26 has the maximum S/N of electrical power as a starting condition. It compares with the three different optimization methods using Taguchi's predictive S/N, as shown in Table 11. The results indicate that the intelligent parameter design via the average PRQL was greater than the starting condition by 32.35%. However, the Taguchi method and the PCA were improved by 32.03% and 31.61%, respectively.

5. Perform Confirmation Experiments

The purpose of the confirmation experiment is to verify whether the conclusions derived from the foregoing data analysis are correct. If the observational results exhibited a great deal of inconsistency between the confirmation experiment and the expected data, this would mean that the experiment failed. Consequently, the previous analysis from the three different optimization methods was used as the basis by which to conduct the confirmation experiments. As shown in Fig. 13, the anode and cathode pressure drop was significantly reduced, but the electrical power was only a decrease by a small amount. For the laminar flow, $\Delta p/\rho = h_l \propto \bar{V} \propto Q$, and for the rest of the turbulent region, $\Delta p/\rho = h_l \propto$ between $\bar{V}$ and $\bar{V}^2$, that is, $Q \sim Q^2$ [34], where h_l is the major head loss, Δp the pressure drop; $\bar{V}$ the average flow velocity; ρ the fluid density and Q is the flowrate $Q = \bar{V} \times A$. Therefore, in this

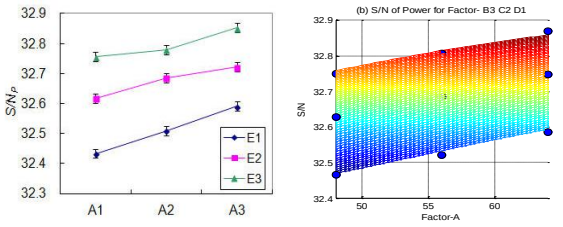

(a) A×E for the electrical power.

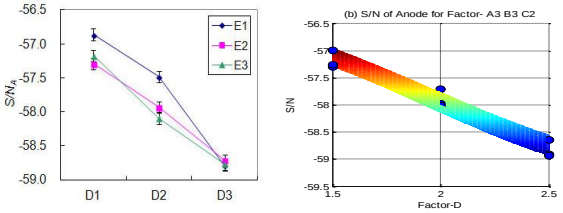

(b) D×E for the anode pressure drop.

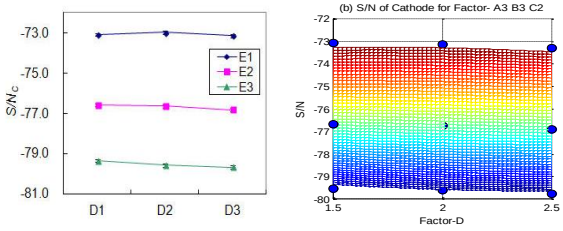

(c) D×E for the cathode pressure drop.

Fig. 11 Comparison of the interaction with Taguchi method and BPNN model for three quality characteristics.

Table 11 Comparison of predictive S/N with the starting condition and three optimal conditions

Factor \ Conditions	Starting Condition			Taguchi Method			PCA Method			BPNN-MC Method		
	$A_3\ B_3\ C_2\ D_2\ E_3$			$A_3\ B_3\ C_2\ D_1\ E_1$			$A_1\ B_1\ C_2\ D_1\ E_1$			—		
Stack temperature (K)	337			337			321			325.75		
Anode humidification temperature (K)	343			343			323			343		
Cathode humidification temperature (K)	333			333			333			342.9		
Stoichiometric hydrogen flow ratio	2			1.5			1.5			1.5		
Stoichiometric airflow ratio	5			2.5			2.5			2.5		
S/N	S/N_P	S/N_A	S/N_C	S/N_P	S/N_A	S/N_C	S/N_P	S/N_A	S/N_C	S/N_P	S/N_A	S/N_C
Predicted	32.87	–58.18	–79.66	32.60	–56.95	–73.16	32.41	–56.79	–73.03	32.51	–56.79	–73.02
Improvement (dB)	0.00	0.00	0.00	-0.26	1.23	6.50	-0.45	1.40	6.63	-0.36	1.39	6.64
PRQL	0.00%	0.00%	0.00%	–6.20%	24.68%	77.61%	–10.93%	27.48%	78.29%	–8.63%	27.36%	78.31%
Total average PRQL	0.00%			32.03%			31.61%			32.35%		

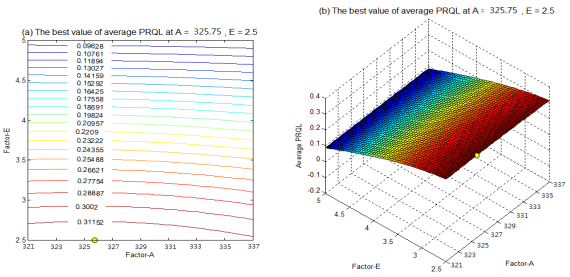

(a) A×E.

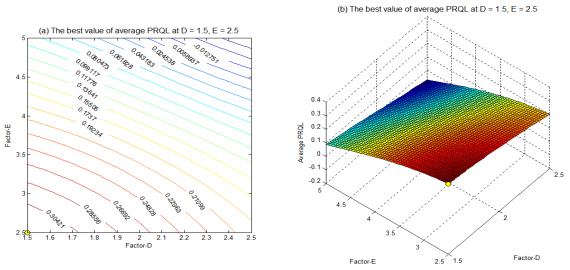

(b) D×E.

Fig. 12 APRQL response of the interaction models for three quality characteristics.

study, applying the pressure drops enables the monitoring of the flow rate and simultaneously meets the demand of the electrical loads. A smaller pressure drop can result in a lower flow rate; that is, a smaller amount of fuel supply or operating cost. In addition, the APRQL for the three different optimization methods are demonstrated to be in good agreement between the confirmation experiments and the predictive results.

CONCLUSIONS

This study presents an integrated approach that combines the fractional factorial DOE, the Taguchi method, the PCA, the BPNN-MC, and the APRQL based on the loss function to optimize the operating conditions for the PEMFC stack. It demonstrates how the intelligent-robust parameter design improves the performance of the PEM fuel cell stack with the three objectives of maximum electric power and minimum anode and cathode pressure drops. In addition, the multi-objective optimization via the APRQL and the PCA handle very important trade-offs among three conflicting objectives.

Based on this study, the following conclusions can be made.

The intelligent parameter design (BPNN-MC) can complement the inadequacy of the Taguchi method and PCA with regard to the best choice for the discrete factor levels. The results indicate that the intelligent parameter design via the average PRQL was greater than the starting condition of a single objective by 32.35%. However, the Taguchi method and the PCA were improved by 32.03% and 31.61%, respectively. The three different optimization methods via APRQL have approximate values that reveal the reliability of the Taguchi method for the choice of the discrete factor levels. Nevertheless, the application of an

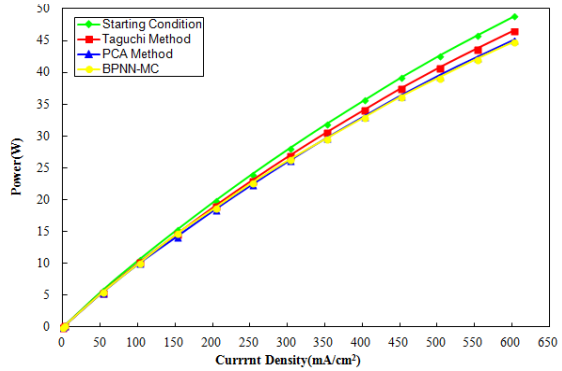

(a) Polarization curve.

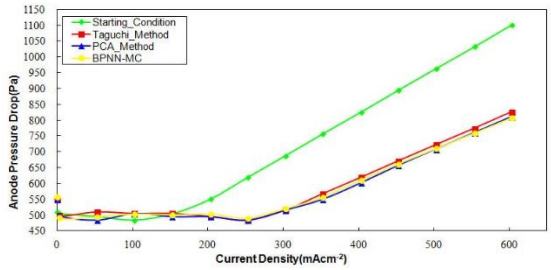

(b) Anode pressure drop.

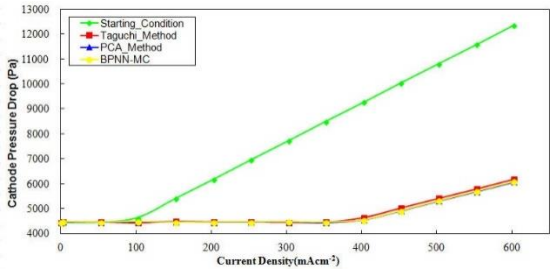

(c) Cathode pressure drop.

Fig. 12 Comparison of the starting condition ($A_3B_3C_2D_2E_3$) and the three optimal conditions.

intelligent parameter design is a more precise method by which to predict the optimal value of the continuous factor levels. Overall, the electrical power is only a decrease by a small amount, but the consumption of gas can save a lot.

Based on this study, we suggest that PEM fuel cell designers and users should consider a compromise between gas costs and electric power by using systematic analysis. Designing or achieving the lowest gas cost according to the use of power requirements is a robust design that takes both cost and efficiency into consideration simultaneously.

PEM fuel cells are popularly applied to the air independent propulsion (AIP) system in submarines. The output power of PEM fuel cell stacks used for AIP system is usually hundreds of kilowatts. In contrast to these large fuel cell stacks, the average power of the PEM fuel cell stack studied in this work is about 45 watts. Hence, the optimum factor-level obtained in this study might not be suitable for those large fuel cell stacks. However, this integrated intelligent-robust parameter design approach presented in this study should be applicable to the large fuel cell stacks in submarine to obtain optimum robust parameter design.

REFERENCES

1. Larminie, J. and J. Dicks, *Fuel Cell Systems Explained*, 2nd ed., John Wiley & Sons, Chichester, West Sussex, UK (2003).
2. Wang, Y., K.S. Chen, J. Mishler, S.C. Cho, and X.C. Adroher, "A review of polymer electrolyte membrane fuel cells: technology, applications, and needs on fundamental research," *Appl. Energy*, Vol. 88, pp. 981-1007 (2011).
3. Wu, H.W., "A review of recent development: transport and performance modeling of PEM fuel cells," *Appl. Energy*, Vol. 165, pp. 81-106 (2016).
4. Sutharssan, T., D. Montalvao, Y.K. Chen, W.C. Wang, C. Pisac, and H. Elemara, "A review on prognostics and health monitoring of proton exchange membrane fuel cell," *Renew. Sust. Energ. Rev.*, Vol. 75, pp. 440-450 (2017).
5. Sinha, V. and S. Mondal, "Recent development on performance modelling and fault diagnosis of fuel cell systems," *Int. J. Dyn. Control.*, Vol. 6, pp. 511-528 (2018).
6. O'Hayre, R., S.W. Cha, W. Colella, and F.B. Prinz, *Fuel Cell Fundamentals*, 2nd ed., Wiley & Sons, New York, USA (2006).
7. Barbir, F., *PEM Fuel Cells: Theory and Practice*, 2th ed., Academic Press, Waltham, MA, USA (2005).
8. Chen, J, and Q. Song, "A decentralized dynamic load power allocation strategy for fuel cell/supercapacitor-based APU of large more electric vehicles," *IEEE Trans. Ind. Electron.*, Vol.66, pp. 865-875 (2019).
9. Aoki, T., S. Tsukioka, H. Yoshida, T. Hyakudome, S. Ishibashi, T. Sawa, J. Ishikawa, A. Tahara, I. Yamamoto, and M. Ohkusu, "Advanced Technologies for Cruising AUV Urashima," *Int. J. Offshore Polar Eng.*, Vol. 18, pp. 81-90 (2008).

10. Hyakudome, T., H. Yoshida, T. Nakatani, Y. Ohta, T. Tani, K. Sugihara, T. Moriga, T. Iwamoto, Y. Kawaharazaki, and T. Oda, "Development of fuel cell system for underwater power source," *OCEANS*, Bergen, Norway (2013).
11. Yu, W.L., S.J. Wu, and S.W. Shiah, "Parametric analysis of the proton exchange membrane fuel cell performance using design of experiments," *Int. J. Hydrog. Energy*, Vol. 33, pp. 2311-2322 (2008).
12. Yu, W.L., S.J. Wu, and S.W. Shiah, "Experimental analysis of dynamic characteristics on the PEM fuel cell stack by using Taguchi approach with neural networks," *Int. J. Hydrog. Energy*, Vol. 35, pp. 11138-11147 (2010).
13. Miao, J.M., S.J. Cheng, and S.J. Wu, "Metamodel based design optimization approach in promoting the performance of proton exchange membrane fuel cells," *Int. J. Hydrog. Energy*, Vol. 36, pp. 15283-15294 (2011).
14. Cheng, S.J., J.M. Miao, and S.J. Wu, "Use of metamodeling optimal approach promotes the performance of proton exchange membrane fuel cell (PEMFC)," A*ppl. Energy*, Vol. 105, pp. 161-169 (2013).
15. Na, W. and B. Gou, "The efficient and economic design of PEM fuel cell systems by multi-objective optimization," *J. Power Sources*, Vol. 166, pp. 411-418 (2007).
16. Ang, S.M.C., D.J.L. Brett, and E.S. Fraga, "A multi-objective optimisation model for a general polymer electrolyte membrane fuel cell system," *J. Power Sources*, Vol. 195, pp. 2754-2763 (2010).
17. Lin, P., P. Zhou, and C. Wu, "Multi-objective topology optimization of end plates of proton exchange membrane fuel cell stacks," *J. Power Sources*, Vol. 196, pp. 1222-1228 (2011).
18. Peng, L., J. Mai, P. Hu, X. Lai, and Z. Lin, "Optimum design of the slotted-interdigitated channels flow field for proton exchange membrane fuel cells with consideration of the gas diffusion layer intrusion," *Renew. Energy*, Vol. 36, pp. 1413-1420 (2011).
19. Shokuhi-Rad, A., A. Jamali, M. Naghashzadegan, N. Nariman-Zadeh, and A. Hajiloo, "Optimum pareto design of non-linear predictive control with multi-design variables for PEM fuel cell," *Int. J. Hydrog. Energy*, Vol. 37, pp. 11244-11254 (2012).
20. Curteanu, S., C.G. Piuleac, J.J. Linares, P. Cañizares, M.A. Rodrigo, and J. Lobato, "Neuro-evolutionary approach applied for optimizing the PEMFC performance," *Int. J. Hydrog. Energy*, Vol. 39, pp. 4037-4043 (2014).
21. Askarzadeh, A. and A. Rezazadeh, "Artificial neural network training using a new efficient optimization algorithm," *Appl. Soft Comput.*, Vol. 13, pp. 1206-1213 (2013).
22. Khaw, J.F., B. Lim, and L.E. Lim, "Optimal design of neural networks using the Taguchi method," *Neurocomputing*, Vol. 7, pp. 225-245 (1995).
23. Su, C.T. and L.I. Tong, "Multi-response robust design by principal component analysis," *Total. Qual. Manag. Bus. Excell.*, Vol. 8, pp. 409-416 (2010).
24. Wu, F.C., "Optimisation of multiple quality characteristics based on percentage reduction of Taguchi's quality loss," *Int. J. Adv. Manuf. Technol.*, Vol. 20, pp. 749-753 (2002).
25. Montgomery, D.C., *Design and Analysis of Experiments*, 7th ed., John Wiley & Sons, Hoboken, NY, USA (2009).
26. Lee, H.H., *Taguchi Methods: Principles and Practices of Quality Design*, 3th ed., Gau Lih Book Co., Taiwan (2011, in Chinese).
27. Matlab, User's Guide, The MathWorks Company (2008).
28. Foresee, F.D. and M.T. Hagan, "Gauss-Newton approximation to Bayesian learning," *Proc. IEEE 1997 Int. Conf. Neural Networks*, pp. 1930-1935 (1997).
29. Wang, G.G. and S. Shan, "Review of metamodeling techniques in support of engineering design optimization," *J. Mech. Design*, Vol .129, pp. 370-380 (2007).
30. Negnevitsky, M., *Artificial Intelligence: A Guide to Intelligent Systems*, 3th ed., Pearson Education, Newmarket, Ontario, Canada (2011).
31. Wu, F.C. and C.C. Chyu, "A Comparative study on Taguchi's SN Ratio, minimising MSD and variance for nominal-the-best characteristic experiment," *Int. J. Adv. Manuf. Technol.*, Vol.20, pp. 655-659 (2002).
32. Kaiser, H.F., "The application of electronic computers to factor analysis," *Educ. Psychol. Meas.*, Vol.20, pp. 141-151 (1960).
33. Yang, T., H.C. Lin, and M.L. Chen, "Metamodeling approach in solving the machine parameters optimization problem using neural network and genetic algorithms:

a case study," *Robot. Comput. Integr. Manuf.*, Vol. 22, pp. 322-331 (2006).

34. Fox, R.W., A.T. McDonald, and P.J. Pritchard, *ntroduction to FluidMechanics*, 7th ed., John Wiley & Sons, Hoboken, NY, USA (2010).

NOMENCLATURE

A	cross section area of flow
a_{k1}, a_{k2}, ...	elements of the eigenvector corresponding to the k-th eigenvalue
$APRQL$	averaged percentage reduction of quality loss
F	value of F-test
F_p	performance function
h_l	major head loss
k	loss coefficient
L_{ij}	loss function for the i-th response at the j-th trial
L_i^+	maximum quality loss for the i-th response
L_i^-	minimum quality loss for the i-th response
MSD	mean square deviation
N_{Hidden}	initial number of hidden node
$PRQL$	percentage reduction of quality loss
Q	Flow rate
R^2	coefficient of determination
$RMSE$	root mean square error
S/N	signal-to-noise ratio
S/N_{LTB}	signal-to-noise ratio for larger-the-better problem
S/N_{STB}	signal-to-noise ratio for smaller-the-better problem
SS_E	sum squared error
SS_w	sum squared weights of the network
V	Degree of resolution
$\bar{V}$	average flow velocity
Y_{ij}	normalized quality loss for the i-th response at the j-th trial
y	value of the quality characteristic
y_i	the i-th observed value
$y_{\max}$	maximum value of the raw data
$y_{\min}$	minimum value of the raw data
y_n	normalized data
$\bar{y}$	mean of the observed value
$\hat{y}_i$	the i-th predicted value
Δp	pressure drop
α, β, ...	performance function parameters
δ	S/N difference between the original and new parametric design
η	signal-to-noise ratio
$\bar{\eta}_{A_iB_j}$	S/N of factorial combination effect
$\bar{\eta}_M$	average S/N for all runs
$\hat{\eta}_M$	predicted S/N
ρ	fluid density
Φ	principal component

應用田口法與智慧型參數設計於 PEM 燃料電池堆多品質性能研究

歐陽寬[*] *李川田*[**] *張瑞珩*[***]

[*]台北海洋科技大學 輪機工程系
[**]國防大學理工學院 國防科學研究所
[***]國防大學理工學院 動力及系統工程學系

關鍵詞：質子交換膜燃料電池堆、田口法、主成份分析法、倒傳遞神經網路、多目標最佳化

摘 要

本研究採用智慧型穩健參數設計方法進行質子交換膜燃料電池堆多品質性能分析，其內容包括：實驗計劃法進行篩選實驗、田口法(Taguchi Method)多品質分析與離散模型預測、主成份分析法(Principal components analysis，PCA)進行統

計上的多目標決策，以及倒傳遞神經網路結合蒙地卡羅法之智慧型參數設計；然後，利用品質損失減少百分率(PRQL)判定最佳參數水準組合，其中探討的操作參數計有電池溫度、陰極與陽極加濕溫度及反應氣體計量比，以達供氣最少，同時輸出電功率最大之多目標性能，最後，由智慧型參數設計、主成份分析法與田口法分別比較電功率最大參數水準組合提升平均品質損失減少百分率(APRQL)為 32.35%、31.61%、32.03%。

(Manuscript received Aug. 19, 2019,
Accepted for publication Feb, 17, 2020)